Induction of Integral Membrane PAM Expression in AtT-20 Cells Alters the Storage and Trafficking of POMC and PC1

Giuseppe D. Ciccotosto,* Martin R. Schiller,‡ Betty A. Eipper,* and Richard E. Mains*

*Departments of Neuroscience and Physiology and ‡Departments of Pathology and Anesthesiology, The Johns Hopkins University School of Medicine, Baltimore, Maryland 21205

Abstract. Peptidylglycine α-amidating monooxygenase (PAM) is an essential enzyme that catalyzes the COOH-terminal amidation of many neuroendocrine peptides. The bifunctional PAM protein contains an NH_2-terminal monooxygenase (PHM) domain followed by a lyase (PAL) domain and a transmembrane domain. The cytosolic tail of PAM interacts with proteins that can affect cytoskeletal organization. A reverse tetracycline-regulated inducible expression system was used to construct an AtT-20 corticotrope cell line capable of inducible PAM-1 expression. Upon induction, cells displayed a time- and dose-dependent increase in enzyme activity, PAM mRNA, and protein. Induction of increased PAM-1 expression produced graded changes in PAM-1 metabolism. Increased expression of PAM-1 also caused decreased immunofluorescent staining for ACTH, a product of proopiomelanocortin (POMC), and prohormone convertase 1 (PC1) in granules at the tips of processes. Expression of PAM-1 resulted in decreased ACTH and PHM secretion in response to secretagogue stimulation, and decreased cleavage of PC1, POMC, and PAM. Increased expression of a soluble form of PAM did not alter POMC and PC1 localization and metabolism. Using the inducible cell line model, we show that expression of integral membrane PAM alters the organization of the actin cytoskeleton. Altered cytoskeletal organization may then influence the trafficking and cleavage of lumenal proteins and eliminate the ability of AtT-20 cells to secrete ACTH in response to a secretagogue.

Key words: rTet • regulated • sorting • granules • actin

PEPTIDYLGLYCINE α-amidating monooxygenase (PAM)[1] is a bifunctional enzyme found in nearly all large dense core vesicles (LDCVs; Eipper et al., 1993). The major forms of PAM are type I integral membrane proteins that catalyze the COOH-terminal amidation of glycine-extended peptides in a two-step process (Eipper et al., 1993; Kolhekar et al., 1997). Peptidylglycine α-hydroxylating monooxygenase (PHM) catalyzes the first step of the reaction, whereas peptidyl-α-hydroxyglycine α-amidating lyase (PAL) catalyzes the second step. The precursor PAM protein, PAM-1 (Fig. 1), is composed of an initial signal and propeptide sequence followed by the PHM catalytic domain, a noncatalytic domain referred to as exon A, the PAL catalytic domain, a transmembrane domain, and a COOH-terminal domain (Yun et al., 1993). The two catalytic domains of PAM can be expressed independently as soluble PHM and PAL, and both domains have been shown to be targeted efficiently to LDCVs (Milgram et al., 1992). In contrast, when integral membrane forms of PAM were expressed in an AtT-20 mouse corticotrope cell line, they were predominantly localized to the trans-Golgi network (TGN) (Milgram et al., 1993, 1994, 1997). The COOH-terminal domain of PAM interacts with proteins that could affect the cytoskeletal organization via their effects on actin and tubulin (Alam et al., 1997).

AtT-20 cells express high levels of proopiomelanocortin (POMC) and prohormone convertase 1 (PC1) while lower but adequate endogenous levels of PAM are present (Thiele and Eipper, 1990; Milgram et al., 1992). PC1, a member of the family of mammalian subtilisin-like prohormone convertases (Bloomquist and Mains, 1993; Seidah et al., 1993; Lindberg and Zhou, 1995; Rouille et al., 1995), has been shown to be important in the initial stages

Address correspondence to Richard E. Mains, Department of Neuroscience, WBSB 907, The Johns Hopkins University School of Medicine, 725 North Wolfe St., Baltimore, MD 21205. Tel.: 410-955-6938. Fax: 410-955-0681. E-mail: dmains@jhmi.edu

1. *Abbreviations used in this paper:* CSFM, complete serum-free medium; Dox, doxycycline; iPAM, inducible PAM; ISG, immature secretory granule; LDCV, large dense core vesicle; NT, nontransfected; PAL, peptidyl-α-hydroxylglycine α-amidating lyase; PAM, peptidylglycine α-amidating monooxygenase; PC1, prohormone convertase 1; PHM, peptidylglycine α-hydroxylating monooxygenase; POMC, proopiomelanocortin; rTet, reverse tetracycline repressor system; TGN, trans-Golgi network.

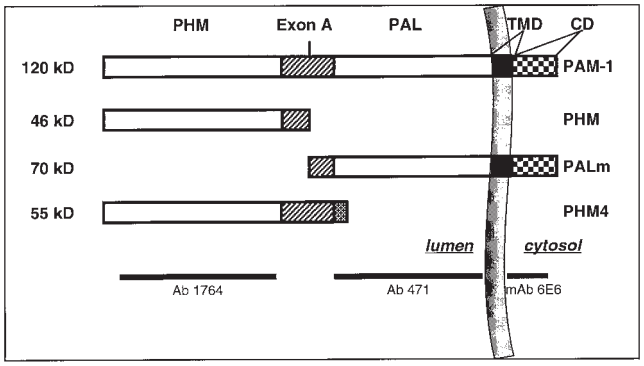

Figure 1. Structures of PAM proteins studied. Intact PAM-1 is an integral membrane protein of 120 kD that consists of two catalytic domains (PHM and PAL) which are separated by the noncatalytic exon A region (hatched box) (Eipper et al., 1993). A proteolytic cleavage site is present within exon A. The PHM and PAL catalytic domains lie within the lumenal compartment. The major protein products generated from PAM-1 cleavage in neuroendocrine cells are 46-kD PHM (soluble) and 70-kD PAL (membrane bound, PALm); PALm includes a transmembrane domain (TMD) and a cytoplasmic domain (CD). PHM4 is a soluble, naturally occurring, alternatively spliced variant of PAM (previously called PAM-4); PHM4 contains the PHM and exon A domains followed by a unique COOH terminus. AtT-20 cells stably transfected with vectors encoding PAM-1 and PHM4 were examined. The specificities of the PAM antisera used in this study are shown. mAb, mouse monoclonal antibody; Ab, rabbit polyclonal antibody.

of POMC processing (Benjannet et al., 1991; Bloomquist et al., 1991; Thomas et al., 1991; Zhou and Mains, 1994). Decreasing PC1 expression in several cell types, by applying the antisense RNA approach, blocked propeptide processing at the early steps (Bloomquist et al., 1991; Eskeland et al., 1996; Yoon and Beinfeld, 1997) while overexpressing PC1 in AtT-20 cells was associated with an increased rate of POMC cleavage and a more extensive cleavage of POMC to smaller products (Zhou and Mains, 1994).

Processing of propeptides begins in the TGN and further processing occurs in immature granules (Schnabel et al., 1989; Paquet et al., 1994; Hendy et al., 1995; Patel and Galanopoulou, 1995). Peptide products are concentrated and packaged into LDCVs which are stored and then released upon stimulation (Milgram et al., 1992; Steiner et al., 1996). The mechanisms underlying the sorting and packaging of POMC products are controversial. It has been proposed that a sorting motif in POMC binds to a sorting receptor such as carboxypeptidase E (Cool et al., 1997; Shen and Loh, 1997; Normant and Loh, 1998). However, other studies have concluded that proteins move from the TGN into immature granules and are subsequently sorted (Irminger et al., 1997; Kuliawat et al., 1997; Thiele et al., 1997; Udupi et al., 1997; Varlamov et al., 1997; Klumperman et al., 1998). Chromogranin B has been proposed to function as a helper protein in the sorting of products to secretory granules (Natori and Huttner, 1996). It is thought that the presence of a highly conserved disulfide-bonded loop structure is essential for sorting of chromogranin B (Huttner et al., 1995). Other factors that may be important in the sorting and packaging of secretory granule products include the specific parameters of the luminal milieu such as pH and calcium concentration (Chanat et al., 1991; Colomer et al., 1996; Kromer et al., 1998).

Previously, we noted that overexpression of integral membrane PAM was associated with an increased release of intact POMC and its first cleavage product (ACTH biosynthetic intermediate), in an unregulated ("constitutive-like") manner (Mains et al., 1991; Milgram et al., 1992). However, the use of clonal cell lines could not establish a causal relationship for this observation, due to possible differences attributable to clonal variation. Since soluble PAM aggregates with some other soluble LDCV proteins (Colomer et al., 1996), the effects of membrane PAM overexpression could involve lumenal interactions. Alternatively, saturation of limiting amounts of cytoplasmic targeting proteins or disrupted signaling to cytoskeletal effectors could have important consequences for trafficking of peptide-containing vesicles (Leube et al., 1994).

To avoid clonal variation as a possible explanation for differences between nontransfected cells and any one particular transfected cell line, the inducible reverse tetracycline repressor system (rTet) of Gossen and Bujard was developed for membrane PAM (Gossen et al., 1993, 1994; Schiller et al., 1997). Using this system, we examined two issues: whether PAM processing and trafficking are saturable and, secondly, whether increasing expression of PAM affects ACTH or PC1 trafficking, processing, and regulated secretion. We demonstrate that the effects of membrane PAM on ACTH and PC1 storage and secretion may be mediated through its effects on cytoskeletal organization.

Materials and Methods

Generation of Stable Cell Lines

An AtT-20 cell line, engineered for inducible PAM (iPAM) expression using the rTet has been described previously (Gossen et al., 1993, 1994; Schiller et al., 1997). AtT-20/D-16v cells (Milgram et al., 1992) were initially transfected with pUHD17-2.neo, selected with G418 (0.5 mg/ml; Sigma) and screened by slot blot and Northern blot for RNA using a rtTA cDNA probe. Clonal pUHD cell lines were obtained by subcloning and screened by in situ hybridization (Schiller et al., 1997). The pUHD.PAM vector was cotransfected into AtT-20/pUHD cells with pSCEP to confer hygromycin resistance (Paquet et al., 1996). Cells containing all three plasmids were selected by growth in medium containing G418 (0.1 mg/ml) and hygromycin (200 U/ml; Sigma) and were subcloned as required. The resulting iPAM cell lines were evaluated by immunostaining with PAM antisera. Cell lines were maintained in DME/F12 medium containing sera from donor herds (10% defined equine serum; Hyclone Laboratories) in an atmosphere of 95% air, 5% CO_2. Nontransfected cells and cell lines stably expressing pUHD, PAM-1, or PHM4 were maintained as previously described (Milgram et al., 1992). A new stable PAM-1 line was also generated for this study using a different vector (pCI.neo) but with identical properties to the original cell line.

iPAM cells were treated with the antibiotic doxycycline (Dox) to induce PAM expression. The health and viability of the cells were normal up to 4 μg/ml Dox, but treatment with 8 μg/ml Dox was associated with decreased PAM protein and enzymatic activity and rounding up of the cells. To determine the optimal treatment time for Dox induction of PAM expression, iPAM cells were treated with a maximally effective dose of Dox (4 μg/ml) for varying time periods. Using antisera to PHM and PAL, increased levels of PAM protein were first detectable after 8 h of Dox treatment. Peak levels of PAM protein were observed after 48 h of Dox treatment and longer treatment of iPAM cells (72 or 96 h) did not alter

the PAM expression levels in these cells (data not shown). In addition, iPAM cells treated for up to 14 d with optimal doses of Dox showed no apparent detrimental effects (data not shown). Removal of Dox from iPAM cells treated with 4 μg/ml Dox for 48 h slowly restored PAM expression to basal levels (data not shown); 24 h after removal of Dox there was no decline in PAM expression. Dox had no noticeable effect on nontransfected cells under the same conditions used for induction of iPAM cells (data not shown).

Antibodies

Polyclonal rabbit antisera raised to different regions of PAM were used: Ab1764 (rPAM-1[37-382]) detected PHM; Ab471 (rPAM-1[464-864]) detected PAL (Milgram et al., 1992). mAb 6E6 (rPAM-1[898-976]) detected the cytoplasmic domain of rPAM-1 and mAb 18E5 detected the PHM domain (Yun et al., 1993; Milgram et al., 1997). Other rabbit polyclonal antisera used detected the NH_2-terminal region of ACTH (JH93; Zhou et al., 1993), PC1[359-373] (JH888; Zhou and Mains, 1994), and TGN38[155-249] (JH1479; Milgram et al., 1997). Rabbit antisera were raised at Covance.

Northern Blot Analysis

Total RNA was isolated using RNA Stat-60 reagent (TelTest B) and fractionated using denaturing formaldehyde gels. PAM mRNA was visualized using a PHM probe (1.3-kb PstI-BamHI fragment of rPAM-1, nt 356-1682; Thiele and Eipper, 1990). RNA loading was normalized using a probe for the ribosomal protein S26 (Vincent et al., 1993).

Western Blot Analysis

Cell extracts or conditioned media were fractionated on either 10 or 12% polyacrylamide, 0.25% *N*,*N*′-methylene-bis-acrylamide/SDS slab gels, transferred to Immobilon-P membranes (Millipore) and visualized using the enhanced chemiluminescence kit (Amersham Lifescience) (Husten and Eipper, 1991; Milgram et al., 1992). Densitometric analysis of the immunoblots was performed using NIH Image analysis software (National Institute of Mental Health) (Milgram et al., 1993).

Cell Extracts and PAM Enzyme Assays

Cells were scraped into ice-cold 20 mM Na(*N*-tris[hydroxymethyl]methyl-2-aminoethanesulfonic acid) (NaTES)/10 mM mannitol, pH 7.4, 1% Triton X-100 (TMT), containing protease inhibitors (Milgram et al., 1992). After three cycles of freezing and thawing, the supernatant was retained and the pellet was discarded. Protein concentrations were determined using the bicinchoninic acid protein reagent kit (Pierce Chemical Co.). PHM and PAL assays were performed on cell extracts as previously described using acetyl-Tyr-Val-Gly and acetyl-Tyr-Val-α-hydroxyglycine as substrates, respectively (Kolhekar et al., 1997).

Biosynthetic Labeling and Immunoprecipitation

Cells were plated on 12-mm culture dishes coated with 0.1 mg/ml poly-L-lysine (Sigma) and grown for 48 to 72 h before biosynthetic labeling. Cells were incubated for 10 min in complete serum-free medium (CSFM) lacking methionine (selectamine kit; GIBCO BRL), then labeled for 30 min with 250 μCi [^{35}S]methionine (~1 μM [Met]; Amersham) at 37°C in air atmosphere. Cells were chased in CSFM containing 140 μM methionine, 2 mg/ml BSA, 0.1 mg/ml lima bean trypsin inhibitor, pH 7.4, for different time periods. After the chase periods, the spent medium was collected, centrifuged at 2,000 *g* to pellet nonadherent cells, and the supernatant was transferred to a new tube containing a cocktail of protease inhibitors (Milgram et al., 1992). All samples were kept at −80°C until further analysis. Cell extracts (5×10^6 dpm, trichloroacetic acid precipitable) and equivalent amounts of spent media were subjected to immunoprecipitation using a rabbit polyclonal antiserum to PAM. Immune complexes were collected with protein A beads and analyzed by SDS-PAGE followed by fluorography (Zhou et al., 1993).

Secretion of ACTH Immunoreactivity

Duplicate wells of cells (nontransfected and stably transfected PAM-1, iPAM−, iPAM+, pUHD−, and pUHD+) were plated on poly-L-lysine–treated wells for measurements of ACTH secretion. Wells were initially rinsed for three 30-min periods in basal release medium (DME/F12/Air with 2 mg/ml fatty acid–free BSA, 0.1 mg/ml lima bean trypsin inhibitor, 1 μg/ml insulin, 0.1 μg/ml transferrin) (Mains and Eipper, 1981; Milgram et al., 1993). The experiment was begun with two successive 30-min basal collections taken using control medium and concluded with one 30-min period of stimulated secretion (1 mM $BaCl_2$ in basal release medium). The collected medium was centrifuged to remove nonadherent cells and protease inhibitors were added and the medium frozen until assay. Cells were extracted using 5 N acetic acid with protease inhibitors, lyophilized, and then dissolved in radioimmunoassay buffer with protease inhibitors. ACTH radioimmunoassays were performed using Ab Kathy (1:15,000) and [^{125}I]ACTH(1-39) (Amersham); this antiserum only recognizes POMC products in which the COOH-terminal end of ACTH(1-39) is exposed (Schnabel et al., 1989).

Immunofluorescence Staining for Filamentous Actin

To detect filamentous actin, cells were fixed in prewarmed 4% paraformaldehyde for 20 min, washed once with PBS (50 mM sodium phosphate, 150 mM sodium chloride, pH 7.4), permeabilized for 20 min (0.075% Triton X-100, 2 mg/ml BSA in PBS), washed once, and incubated in block for 30 min (2 mg/ml BSA in PBS). Cells were incubated with a PAM mAb (6E6) for 120 min, then washed three times with PBS. PAM staining was detected with a donkey anti–mouse Cy3 and filamentous actin visualized with a 1.2 μg/ml FITC-phalloidin. The cells were exposed to this second set of antibodies for 60 min (in the dark), washed three times in PBS, and then mounted with prewarmed DABCO/permount and coverslipped.

Immunofluorescence Staining for PAM, ACTH, TGN38, and PC1

Cells were plated on poly-L-lysine–coated glass chamber slides (Lab-Tek) 48–96 h before fixation. Cells were double immunostained for PAM and ACTH, PAM and TGN38, or for PAM and PC1 as described (Milgram et al., 1997). Cells were viewed under epifluorescence optics with an upright microscope (Axioskop; Zeiss, Inc.) using FITC (BP 485/20, barrier filter 520-560) and rhodamine (BP 546/12, LP 590) filters with an HBO 100-W mercury lamp and a ×40 or ×63 objective lens. Images were photographed using a Micromax digital camera with Winview 3.2 software (Princeton Instruments). One set of images was visualized on a confocal laser microscope (Noran OZ; Noran) at an excitation wavelength of 488 nm (FITC-nar, barrier filter 525 ± 50) and 568 nm (Rho-nar, barrier filter 605 ± 55) from a Krypton-Argon multi-line laser. Z-axis images were processed using Intervision 1.6 software (Noran). A second set of images was visualized on a confocal laser microscope (MRC 600; Bio-Rad Laboratories) at an excitation wavelength of 488 nm (FITC-nar, barrier filter 510-515) and 568 nm (Rho, barrier filter 585) from a Krypton-Argon laser. Z-axis images were processed using Comos 6.05 software. Photographs of nontransfected and transfected cells were taken under identical conditions and printed in an identical fashion. A set of control experiments (omission of primary antibody or omission of secondary antibody) was performed showing that there was no bleed through from one fluorophore into the other filter when appropriate dilutions of antisera were used for double immunostaining.

Results

Dose–Response Curve for Dox Induction of PAM as Determined by Northern Blot Analysis

Induction of PAM-1 mRNA was examined by Northern blot (Fig. 2). iPAM cells were treated with increasing concentrations of Dox for 48 h. In the exposure shown, there is no detectable PAM mRNA in the absence of Dox and the intensity of the signal increases with higher doses of Dox, reaching maximal expression levels at 1–4 μg/ml Dox. With longer exposure times, the level of PAM mRNA in the noninduced iPAM cells was found to be similar to the level of endogenous PAM mRNA in the nontransfected cells (data not shown). There was a 60-fold induction of PAM mRNA expression in the maximally induced iPAM cells compared with the noninduced cells. No decrease in PAM-1 mRNA level was observed with the

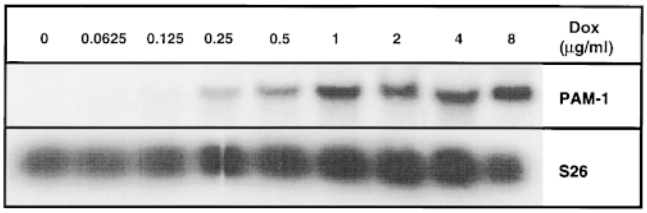

Figure 2. Induction of PAM mRNA in iPAM cells. Northern blot of total RNA (10 μg) isolated from iPAM cells after treatment with the indicated doses of Dox (μg/ml) for 48 h. The membrane was hybridized with cDNA probes for PHM (top) and S26 ribosomal protein (bottom). Similar results were obtained in two other analyses of this type.

highest dose of Dox (8 μg/ml). The level of PAM-1 mRNA in the maximally induced cells was similar to the level in stably transfected PAM-1 cells (data not shown).

Dose–Response Curve for Induction of PAM Protein in iPAM Cells: PHM

Since one of our goals was to examine cells expressing different levels of PAM-1, iPAM cells were treated for 48 h with increasing concentrations of Dox and compared with control cells using enzyme assays (Fig. 3 A) and Western blots (Fig. 3, B and C). Controls included nontransfected AtT-20 cells as well as AtT-20 cells expressing only the reverse tetracycline repressor (pUHD−, untreated; pUHD+, treated with 4 μg/ml Dox for 48 h) or expressing PAM-1 or PHM4. As with PAM mRNA (Fig. 2), Dox exerted a dose-dependent effect on PHM activity (Fig. 3 A). Peak levels of PHM specific activity were observed after treatment with 1–4 μg/ml of Dox. PHM specific activity in the noninduced iPAM cells was similar to nontransfected cells, untreated, and Dox-treated pUHD cells (Fig. 3 A). The PHM specific activity of maximally induced iPAM cells was 20–30-fold higher than noninduced iPAM cells and comparable to that of the stably transfected PAM-1 and PHM4 cells (Fig. 3 A). The sensitivity of iPAM cells to induction with low amounts of Dox can be seen by the two- to fivefold increase in PHM specific activity when noninduced cells are compared with cells treated with 0.0625 μg/ml Dox.

Increasing concentrations of Dox produced a dose-dependent increase in PAM protein expression in the iPAM cells (Fig. 3 B). Intact PAM-1 (120 kD) and soluble PHM (46 kD) were apparent in the Dox-treated iPAM cells as in the stably transfected PAM-1 cells (Fig. 3 B). Since 46-kD PHM can be stored or secreted, spent media were also examined (Fig. 3 C). Cells were incubated in CSFM for 6 h; equal amounts of cell protein (Fig. 3 B) and a 10-fold higher volume of spent medium (representing secretion) (Fig. 3 C) were visualized with an antiserum to PHM. Due to the limited sensitivity of our antisera, endogenous PAM expression in iPAM cell extracts before induction (0 Dox) or in nontransfected cells, pUHD−, and pUHD+ cells is not detectable (Fig. 3 B). The addition of Dox (4 μg/ml for 48 h) to the culture medium of nontransfected and PAM-1 cells had no effect on PAM protein expression (data not shown).

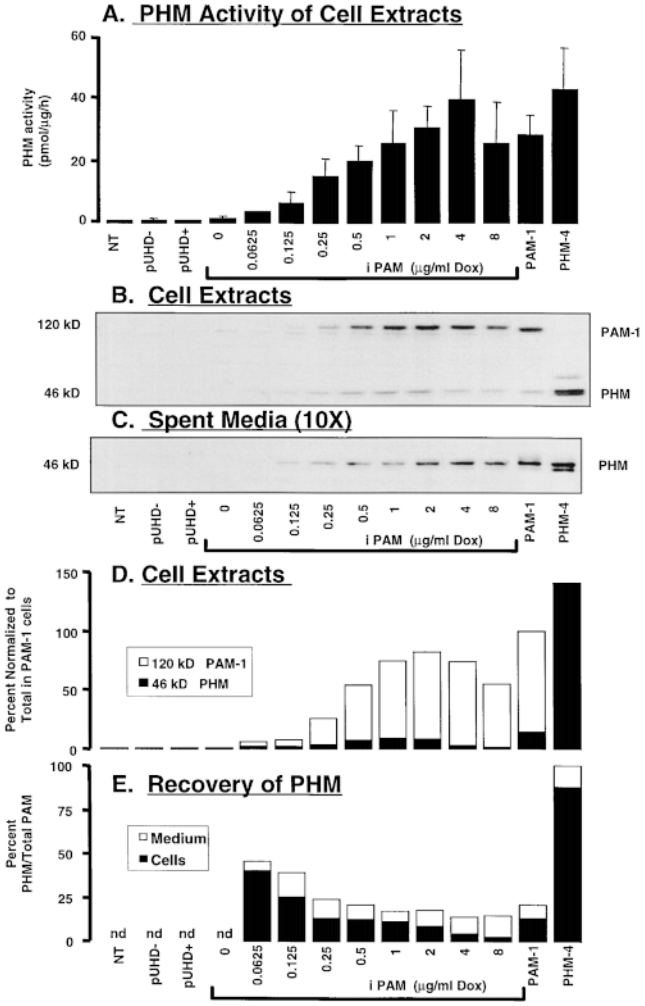

Figure 3. Induction of PAM protein in iPAM cells: PHM analysis. A dose–response curve was generated by incubating the iPAM cells with the indicated doses of Dox (micrograms per milliliter) for 48 h. NT and stably transfected pUHD−, pUHD+ (treated with 4 μg/ml Dox for 48 h), PAM-1, and PHM4 cell lines were also analyzed. (A) PHM specific activity was measured in cell extracts (mean ± SEM; n = 2–4). Western blots of 20 μg of cell protein (B) and spent medium corresponding to 200 μg cell protein (6 h basal collection, C) were visualized with antiserum to PHM (Ab 1764). (D) Blots from cell extracts were digitized; expression in PAM-1 cells was set to 100%, and the relative contributions of intact 120-kD PAM-1 (open bars) and 46-kD PHM (filled bars) are plotted as a stacked bar graph. (E) For each cell line or dose of Dox-treated cells, the amount of 46-kD PHM in cell extracts (B) or spent medium (C) (taking into account the 10-fold excess volume analyzed) was expressed as a percentage of total PAM; total PAM = 120-kD PAM-1 (cells) + 46-kD PHM (cells and media). Similar results were obtained in two additional experiments.

Maximum PAM protein levels in the iPAM cell line (1–4 μg/ml Dox) were similar to levels in the stably transfected PAM-1 cell line and at least 35–40-fold higher than in the noninduced iPAM cells. Western blots of cell extracts and media were digitized (Fig. 3, D and E). In the iPAM cells, the proportion of 46-kD PHM to the total amount of PAM protein in the cell extract decreased 37%

with increasing PAM protein expression (Fig. 3 D). The decreased fraction of 46-kD PHM with increased total cellular PAM expression could reflect decreased cleavage of PAM-1 or increased secretion of 46-kD PHM.

Secretion of PHM from iPAM cells was detectable with Dox doses of 0.0625 μg/ml or higher (Fig. 3 E). At the lowest doses of Dox, more 46-kD PHM was in the cells (filled bars) than in the medium (open bars) after the 6-h basal collection. AtT-20 cells producing soluble PHM (PHM4) store this protein much more efficiently than AtT-20 cells that produce soluble PHM from membrane PAM. As expression of PAM-1 increases, the recovery of 46-kD PHM decreased (Fig. 3 D) and the fraction of the 46-kD PHM recovered in the medium increased (Fig. 3 E). As a result, the amount of secreted 46-kD PHM was similar at the higher levels of induction (>2 μg/ml Dox). The decrease in steady-state levels of 46-kD PHM with increasing levels of PAM-1 expression demonstrates that there are saturable steps in PAM-1 metabolism. In addition, the ability of the cells to store the 46-kD PHM that is produced declines as expression of PAM-1 increases.

Dose–Response Curve for Induction of PAM Protein in iPAM Cells: PAL

As with the PAM mRNA, PHM protein expression, and PHM enzyme activity, a dose-dependent effect of Dox on PAL enzyme activity was observed (Fig. 4 A). Increased expression of PAL activity was apparent with the lowest doses of Dox tested. Peak levels of PAL specific activity were observed after treatment with 2–4 μg/ml Dox; treatment with 8 μg/ml Dox resulted in decreased PAL activity. PAL specific activity in the noninduced iPAM cells was similar to nontransfected, untreated, and Dox-treated pUHD cells (Fig. 4 A). The PAL specific activity of maximally induced iPAM cells was comparable to that of the stably transfected PAM-1 cells and two- to threefold higher than PHM specific activity, reflecting the higher enzymatic turnover rate of PAL (Eipper et al., 1993).

Processing of PAM-1 in the iPAM cells yields a 70-kD PALm product, as in stably transfected PAM-1 cells (Fig. 4 B). A dose-dependent increase in PAM protein expression was seen in the iPAM cells using the PAL antiserum, with levels approaching those in PAM-1 cells; very little soluble PAL is produced from PAM-1 in AtT-20 cells, so Western blots of PAL in spent media are not shown. Western blots were digitized so levels of expression could be compared (Fig. 4 C). The fraction of the total PAM protein in the cell extracts accounted for by 70-kD PALm increased twofold with increasing PAM expression levels (Fig. 4 D). PAM-1 metabolism is clearly altered as a function of expression level.

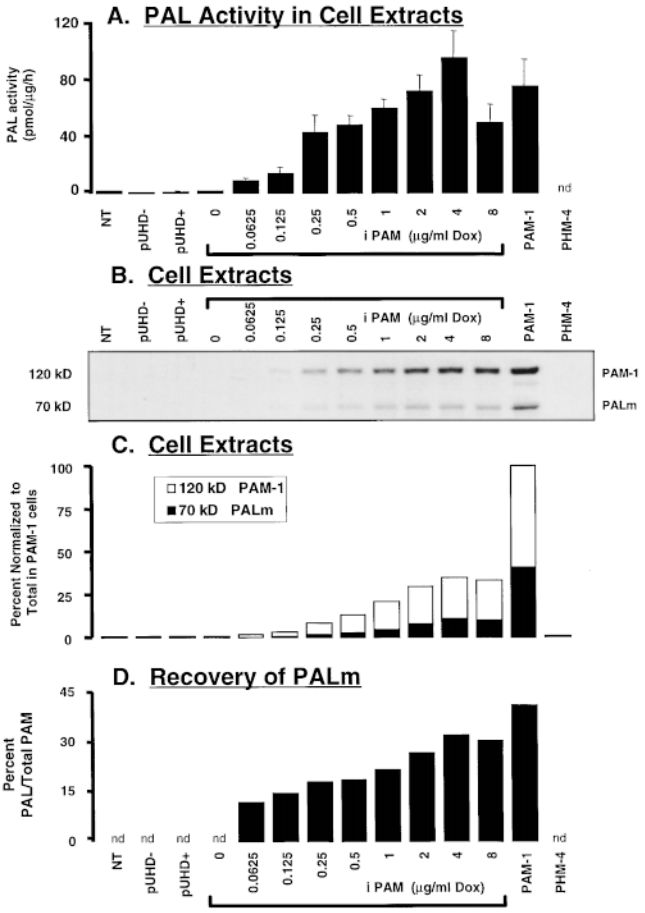

Figure 4. Induction of PAM protein in iPAM cells: PAL analysis. (A) PAL specific activity was measured in cell extracts prepared as described in Fig. 3 (mean ± SEM; n = 2–4). (B) Western blots were carried out on cell extracts using antisera to PAL. (C) Blots were digitized; expression in PAM-1 cells was set to 100% and the relative amounts of PAM-1 (open bars) and 70-kD PALm (filled bars) are plotted as a stacked bar graph. (D) For each cell line or dose of Dox-treated cells, the amount of 70-kD PAL in the cell extract is expressed as a percentage of the total PAM protein in the extract; total PAM = 120-kD PAM-1 (cells) + 70-kD PAL (cells). Similar results were obtained in two additional experiments.

Biosynthesis of PAM-1

The alterations in steady-state levels of PHM and PAL with increasing levels of PAM expression could reflect differences in the rate of biosynthesis of PAM-1, cleavage of PAM-1, degradation, and/or secretion of PHM and PAL. To distinguish these possibilities, identical wells of iPAM cells treated with a low dose of Dox (0.25 μg/ml) or a high dose of Dox (2.0 μg/ml) were incubated in medium containing [^{35}S]Met for 30 min and either harvested immediately (pulse) or chased in medium containing unlabeled Met (chase). PAM proteins immunoprecipitated from cell extracts and media were fractionated by SDS-PAGE (Fig. 5). Consistent with the steady-state levels of PHM and PAL protein and enzyme activity (Figs. 3 and 4), the rate of PAM-1 biosynthesis was 2.8 ± 0.4-fold higher (P < 0.005; n = 4) in cells induced with the high dose of Dox than in cells induced with the low dose of Dox.

Consistent with Western blot analysis (Fig. 3), relative secretion of 46-kD PHM was enhanced when levels of PAM-1 expression were higher. With the low dose of Dox, 65% of the 46-kD PHM present after a 4-h chase was recovered in the medium. In contrast, with the high dose of Dox, 81% of the 46-kD PHM was recovered in the medium. No detectable degradation of PAM protein occurred within 4 h at either level of PAM expression. The

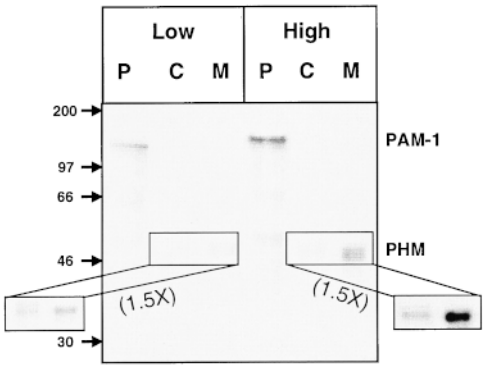

Figure 5. Biosynthesis of PAM after Dox induction. Identical wells of iPAM cells were treated with 0.25 or 2.0 μg/ml Dox for 48 h and then incubated with [^{35}S]Met for 30 min and either harvested immediately (pulse, P) or chased for 0.5, 2, or 4 h (chase); for chase samples, cell extracts (C) and media (M) were analyzed. PAM proteins were immunoprecipitated using antisera to PHM or PAL (not shown); only data for PHM immunoprecipitates from the pulse and 4-h chase samples are shown. (Inset) Longer exposures of films of chase samples are shown.

higher levels of 70-kD PALm observed in PAM-1 cells induced with high levels of Dox may reflect a small change in the turnover rate of this membrane protein.

Localization of PAM-1 and ACTH

To evaluate the localization of PAM at different levels of expression, a dose–response curve for Dox induction of PAM-1 in iPAM cells was examined by immunofluorescence (Fig. 6 A). Cells were fixed and visualized with a mAb directed against the PAM-1 COOH terminus. Less than 1% of the cells stained for PAM-1 when the untreated iPAM cells were examined (Fig. 6 A, 0 Dox); as for Western blots, our antisera cannot detect the endogenous levels of PAM in AtT-20 cells. In iPAM cells treated for 48 h at a low Dox dose (0.25 μg/ml), PAM-1 signal was seen in ~50% of the cells (Fig. 6 A, 0.25 Dox). In maximally induced iPAM cells (4 μg/ml Dox), PAM staining was much more intense and >95% of the cells displayed fluorescence (Fig. 6 A, 4 Dox).

Maximally induced iPAM cells were coimmunostained with antisera for a TGN marker protein (TGN38) and PAM-1 (Fig. 6 B). In the panels shown, two cells show intense PAM-1 staining (green) in the perinuclear region with lighter staining in vesicular structures at the tips of processes (arrows). When the PAM-1 and TGN38 images were superimposed, the TGN region was predominantly yellow, indicating that much of the PAM-1 is localized to the TGN region (Fig. 6 B); TGN staining was not apparent at the tips of the processes (arrows). In a third cell that stained only faintly for PAM-1, the TGN staining pattern was similar to the staining pattern seen in cells expressing more PAM-1 (Fig. 6 B).

Having established that the iPAM cells can be used effectively to control the expression of PAM in a given cell population, the effects of increased PAM expression on ACTH localization were evaluated by immunofluorescence (Figs. 6 C and 7). Fig. 7 shows epifluorescence images of populations of nontransfected and PAM-1–expressing cells whereas Fig. 6 C shows confocal images of two cells among a population of iPAM cells treated with Dox; as occasionally happens, only one of the pair of cells is expressing high levels of PAM (green). In the population of nontransfected (NT) cells (Fig. 7, left), vesicular, punctate staining for ACTH is observed throughout the cytosol with increased staining in the cellular processes and a slight increase in ACTH staining in the TGN region. In the single iPAM cell not expressing high levels of PAM (Fig. 6 C, left cell), the ACTH (red) staining pattern is similar to that of the nontransfected cells. pUHD cells treated with Dox also displayed ACTH staining patterns similar to those seen for nontransfected cells (data not shown). Interestingly, in the confocal image of the iPAM cell expressing PAM-1 (Fig. 6 C, right), the ACTH distribution is dramatically altered, with marked localization of ACTH to the TGN region of the cell and less intense staining of processes. Similar patterns of ACTH staining are observed in the population of AtT-20 cells expressing PAM-1 (Fig. 7, middle). The PAM and ACTH staining patterns of the Dox-treated iPAM cells (Fig. 6 C, right cell) are almost identical to those of the stably transfected PAM-1 cells (Fig. 7, PAM-1).

Confocal microscopy allowed more detailed comparison of the localization of ACTH and PAM in the iPAM+ cells. PAM staining in this cell (Fig. 6 C) is predominantly localized to the TGN region with some staining for PAM at the tips of the cellular processes. When the ACTH and PAM signals are superimposed, a large portion of the TGN region is yellow, consistent with colocalization of ACTH with PAM-1. Compared with the noninduced iPAM cell (Fig. 6 C, left cell), the intensity of ACTH staining is decreased in the cell with increased PAM expression (Fig. 6 C, right cell); a similar difference in staining intensity is seen when comparing ACTH staining in nontransfected and PAM-1 cells (Fig. 7). The different ACTH localization observed in iPAM cells expressing PAM-1 cannot be caused simply by the introduction of proteins into the secretory pathway using the rTet system, since previous results using AtT-20 cells with Dox-inducible expression of regulated endocrine–specific protein of 18 kD showed no effect on POMC biosynthesis or localization (Schiller et al., 1997).

To determine which region of PAM was responsible for altering ACTH localization, nontransfected and stably transfected AtT-20 cell lines expressing either intact PAM-1 or PHM4 (Fig. 7) were compared. In cells expressing PHM4 (lacking the PAL and transmembrane domains of PAM-1), PHM staining differs from that of PAM-1 and iPAM+ cells in that it is primarily seen in the cellular processes with fainter staining in the TGN region (Fig. 7, PHM4). Moreover, the ACTH staining pattern in the PHM4 cells closely resembles that of the nontransfected and noninduced iPAM cells (Figs. 7 and 6 C, left cell, respectively); ACTH staining in the PHM4 cells is primarily seen in the cellular processes with less staining of the TGN region.

Overexpression of PAM-1 Eliminates the Stimulated Secretion of ACTH

Observing that the ACTH immunostaining patterns were

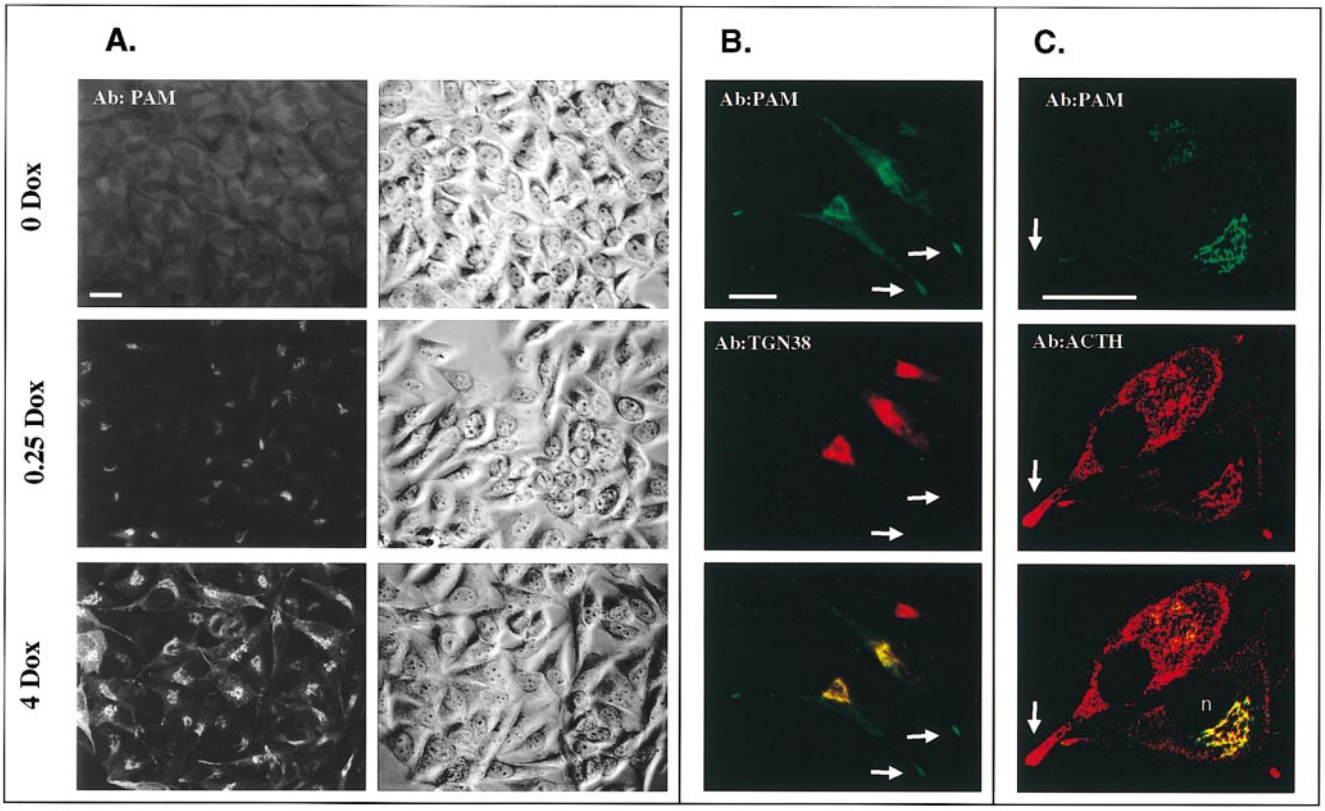

Figure 6. Localization of PAM and ACTH after Dox induction. Immunofluorescent staining for PAM in iPAM cells treated with the indicated doses of Dox (micrograms per milliliter) using mAb 6E6 (A); cells were photographed under identical conditions and the corresponding phase images are shown. (B) Immunofluorescent staining of Dox-treated iPAM cells (4 μg/ml Dox for 48 h) with mAb to PAM (6E6; green) and polyclonal antibody to TGN38 (red); images were taken in black and white and colorized using Adobe Photoshop; areas of overlap appear yellow (bottom). Arrows mark tips of processes. Images in C were obtained with the Noran confocal laser scanning microscope. Dox-treated cells were stained simultaneously for PAM (mAb 6E6; green) and ACTH (JH93; red); the combined images showing areas of PAM and ACTH overlap are seen in yellow (C, bottom). The cell nucleus (n) and tips of cellular processes (arrow) are indicated. Bar, 10 μm.

markedly different in nontransfected cells and cells expressing PAM-1 (Figs. 6 C and 7), their basal and stimulated secretions of ACTH were examined. Secretion of ACTH was quantified using an immunoassay specific for the COOH terminus of ACTH(1-39); secretion was examined during two sequential basal collections and cells were then stimulated with 1 mM $BaCl_2$ (Fig. 8 A). $BaCl_2$ mimics Ca^{2+} and several secretagogues and supports a steady high rate of secretion (Mains and Eipper, 1984). As expected, in nontransfected AtT-20 cells, the addition of secretagogue to the medium stimulated ACTH secretion three- to fourfold above basal levels. A similar fold stimulation of ACTH secretion was observed in control pUHD cells whether or not they were treated with Dox (pUHD−, pUHD+) and in noninduced iPAM cells; none of these cells express exogenous PAM-1. In contrast, in iPAM cells treated with Dox to induce PAM-1 expression, addition of secretagogue to the medium did not stimulate ACTH secretion above basal levels (Fig. 8 A). The effects seen with the iPAM cells cannot be attributable to the Dox treatment alone since the pUHD+ cells responded to secretagogue as well as nontransfected AtT-20 cells or untreated pUHD− cells. As for Dox-treated iPAM cells, secretion of ACTH from stably transfected PAM-1 cells was not stimulated by secretagogue (Fig. 8 A). In contrast, AtT-20 cells expressing a soluble PAM protein (PHM4), exhibited a threefold increase in ACTH secretion in response to secretagogue. Treatment of the iPAM cells with a low, but effective dose of Dox (0.0625 μg/ml) resulted in a partial inhibition of the ability of secretagogue to stimulate ACTH secretion (data not shown). Thus, overexpression of PAM-1 is causally related to the inability of Dox-treated iPAM cells and PAM-1 cells to respond to secretagogue treatment.

In the course of analyzing ACTH secretion by the various AtT-20 cell lines, the utility of having an inducible cell line was clearly apparent (Fig. 8 B). The pUHD cell line selected contained roughly half as much ACTH per milligram of cell protein as the parental, nontransfected AtT-20 cell line. The iPAM cell line subsequently selected contained roughly half as much ACTH per milligram of cell protein as the parental pUHD cell line. In no case did Dox treatment affect the ACTH content of the cells. The PAM-1 and PHM4 AtT-20 lines generated several years ago contained approximately as much ACTH per milligram of cell protein as the newly generated iPAM cell line.

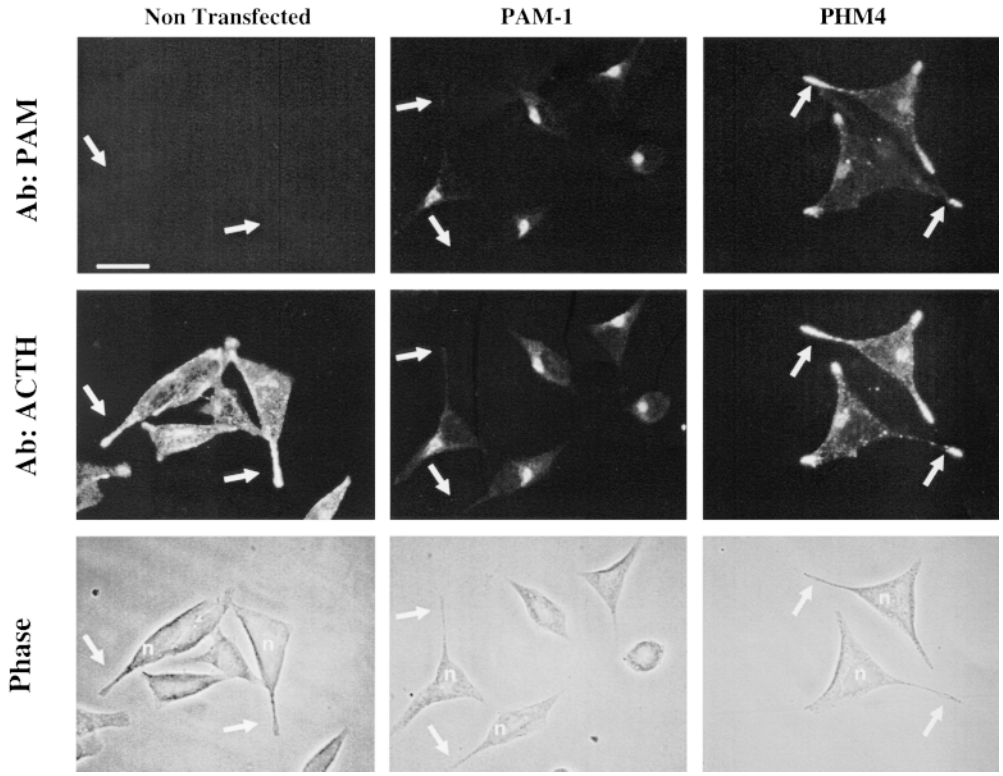

Figure 7. Localization of PAM and ACTH in stable cell lines. Immunofluorescent staining of nontransfected, stably transfected PAM-1 and PHM4 cells for PAM and ACTH (Ab JH93) (6E6 and 18E5, respectively). PAM staining was detected with goat anti–mouse FITC and ACTH staining was visualized with goat anti–rabbit Cy3. Phase-contrast images are also shown. All cells were photographed under identical conditions. The cell nucleus (n) and tips of cellular processes (arrows) are indicated. Bar, 10 μm.

To evaluate regulated secretion of another lumenal protein, the level of PHM activity was determined in the same set of basal and secretagogue stimulated media samples (Fig. 8 C). In the nontransfected AtT-20 cells, the level of PHM activity in the media was sixfold higher after secretagogue stimulation. A similar fold stimulation of secreted PHM activity was observed after secretagogue stimulation of control pUHD cells (whether or not they were treated with Dox [pUHD−, pUHD+]), noninduced iPAM cells, and PHM4 cells. As seen for the ACTH immunoreactivity (Fig. 8 B), cells with increased exogenous PAM-1 expression (iPAM+ and PAM-1 cells) failed to show a robust stimulation of secretion of PHM activity after secretagogue stimulation (only double the basal levels).

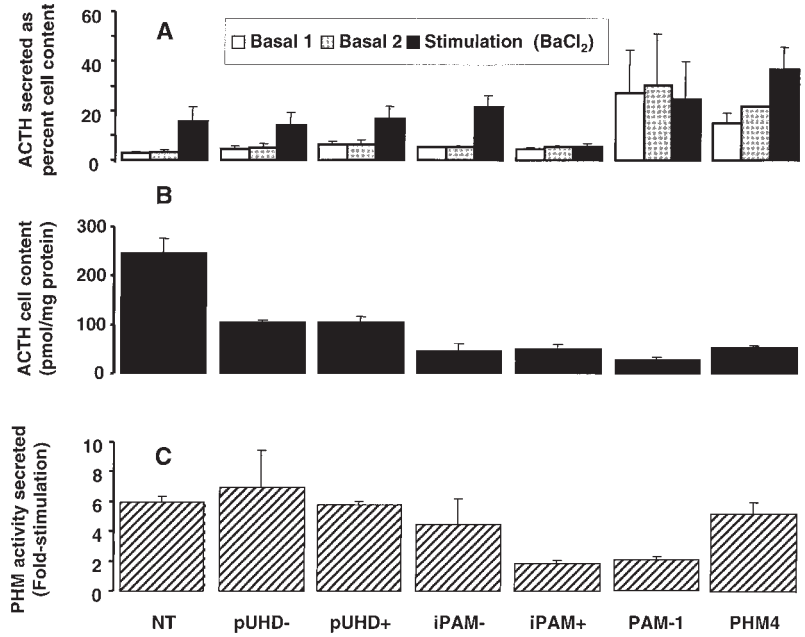

Figure 8. Expression of PAM-1 alters secretion of ACTH in AtT-20 cells. NT and stably transfected pUHD−, pUHD+ (treated with 4 μg/ml Dox for 48 h), iPAM−, iPAM+ (treated with 4 μg/ml Dox for 48 h), PAM-1, and PHM4 cell lines were analyzed as described in Materials and Methods. (A) Medium was collected after two 30-min periods of basal secretion followed by a 30-min period of stimulated secretion (1 mM $BaCl_2$) and the levels of ACTH were determined. (B) Cells were extracted for measurement of total protein and immunoreactive ACTH. Levels of ACTH from duplicate cultures were measured in triplicate (A and B). (C) Medium was collected as in A and assayed for PHM activity. Bars are mean ± SEM.

PC1 Metabolism Is Altered by Increased Expression of PAM-1

To ask whether expression of membrane PAM might affect other LDCV proteins in addition to ACTH, PC1 was investigated. The major products of proPC1 cleavage are mature 82-kD PC1, produced rapidly in the endoplasmic reticulum, and 66-kD PC1ΔC, produced only in LDCVs (Fig. 9 A; Zhou and Mains, 1994). A dose–response curve for Dox induction of PAM-1 expression was generated as described in Figs. 2–4 and cell extracts were subjected to Western blot analysis with antibodies to PC1 (Fig. 9 B). In nontransfected, PHM4, and pUHD− or pUHD+ cells, PC1ΔC was the major form of PC1 in cell extracts. In contrast, in PAM-1 cells, mature 82-kD PC1 predominated in cell extracts. Increasing PAM-1 expression in iPAM cells caused a dose-dependent decrease in the production of PC1ΔC from mature PC1; whereas 65% of the total PC1 was PC1ΔC in noninduced cells, only 30% was PC1ΔC in the maximally induced iPAM cells (Fig. 9 C). PC1ΔC accounted for even less of the total PC1 in stably transfected PAM-1 cells.

PC1 localization was then examined in various PAM cell lines by immunofluorescence (Fig. 9 D). PC1 staining in nontransfected and in noninduced iPAM cells was vesicular and predominantly localized to the tips of the cellular processes (Fig. 9 D, NT and iPAM−). In iPAM cells treated with Dox and expressing high levels of PAM, PC1 was not concentrated at the tips of the processes and there was an overall decrease of PC1 staining intensity. Lack of staining at the tips of processes and decreased PC1 staining intensity were also observed in stably transfected PAM-1 cells. In contrast to the iPAM+ and PAM-1 cells, the PHM4 cells showed prominent PC1 staining at the tips of the cellular processes; the PC1 staining appeared to be colocalized with the PHM staining (Fig. 9 D, PHM4). Thus the PC1 staining pattern of the PHM4 cells more closely resembles that of the nontransfected and iPAM− cells (Fig. 9 D) than the other cells tested.

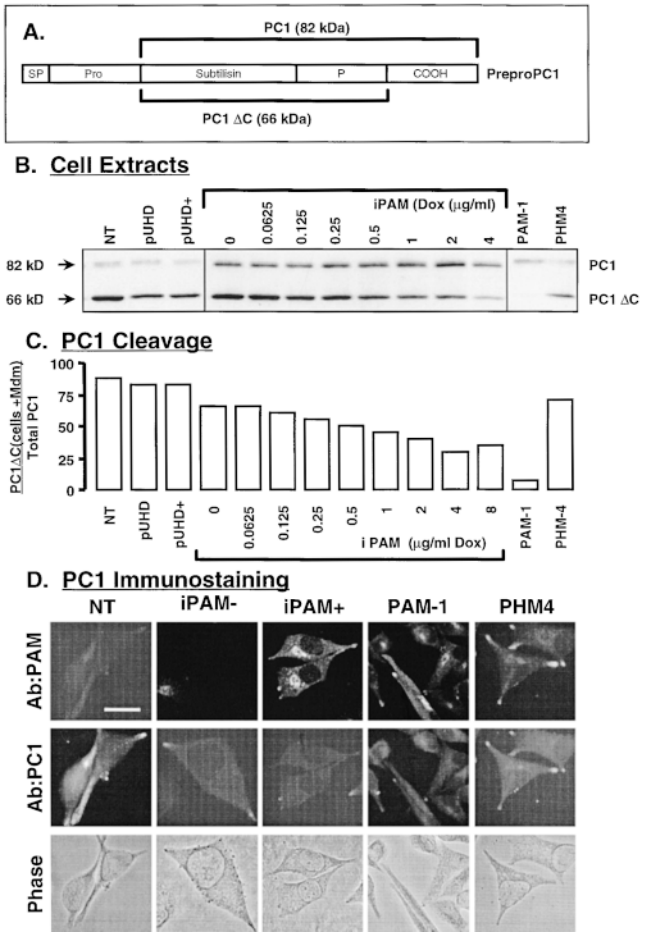

Figure 9. Effect of PAM expression on PC1. (A) Structure of preproPC1; preproPC1 has a signal peptide (SP), proregion (Pro), subtilisin-like catalytic domain (Subtilisin), P-domain (P), and COOH-terminal domain (COOH). ProPC1 (87 kD) is cleaved to yield PC1 (82 kD) and PC1ΔC (66 kD). iPAM cells were treated with the indicated doses of Dox for 48 h. Western blots of 20 μg of cell extracts (B) and spent medium (not shown) were visualized with antiserum to PC1 (Ab JH888). (C) Blots were digitized. (D) Immunofluorescent staining of NT, iPAM−, iPAM+ (treated with 4 μg/ml Dox for 48 h), PAM-1, and PHM4 cells was viewed using phase optics and stained with an antibody for PC1 (Ab JH888). Bar, 10 μm.

Expression of PAM-1 Alters Organization of the Actin Cytoskeleton

Cytoskeletal organization is a powerful factor in regulated exocytosis (Muallem et al., 1995; Carbajal and Vitale, 1997). Since PAM-1 is known to interact with proteins that can indirectly affect cytoskeletal organization (Alam et al., 1997), the distribution of filamentous actin in noninduced and induced iPAM cells was examined using the mushroom toxin, phalloidin (Fig. 10). In noninduced iPAM cells expressing only their endogenous PAM protein, PAM staining was not visible (Fig. 10, iPAM−, red). Filamentous actin was found in clusters broadly distributed throughout the cell and was collected in several subplasma membrane foci (Fig. 10, iPAM−, green); although the edges of the noninduced cells were easily visible, filamentous actin was not enriched in the subplasma membrane region. As expected, after induction with Dox, PAM-1 was largely localized to the TGN region of the cell (Fig. 10, iPAM+, red). A dramatic change in the distribution of filamentous actin accompanied expression of PAM-1 (Fig. 10, iPAM+, green); filamentous actin was concentrated at the plasma membrane with numerous foci of more intense staining. The broadly distributed diffuse patches of filamentous actin were absent from the iPAM+ cells. Patches of filamentous actin were also concentrated in the TGN region of the iPAM+ cells.

Discussion

Characterization of an iPAM Cell Line

PAM is an essential bifunctional enzyme that catalyzes the bioactivation of many peptides (Eipper et al., 1993). The anterior pituitary and atrial myocytes are rich sources of PAM expression (May et al., 1990; Eipper et al., 1993), whereas AtT-20 cells contain lower albeit sufficient levels of PAM to amidate the endogenous substrates. Various

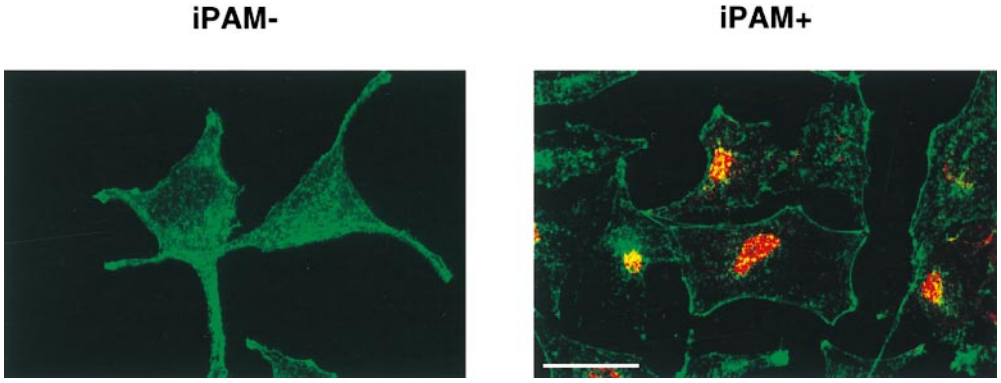

Figure 10. Localization of PAM and filamentous actin after Dox induction. Staining of noninduced iPAM cells (iPAM−) and Dox-treated iPAM cells (iPAM+; 4 μg/ml Dox, 48 h) using a mAb to PAM (6E6; red) and FITC-phalloidin (green). Images were obtained with the Bio-Rad confocal laser scanning microscope. Bar, 25 μm.

forms of PAM have been expressed successfully in AtT-20 cells, with stable expression of membrane PAM reaching levels found in the anterior pituitary (May et al., 1990). The use of stable cell lines is an important tool in addressing many questions relating to peptide processing and sorting, but their limitations include clonal variability and inability to regulate the level of protein expression. This problem is illustrated by the variable ACTH content of the nontransfected, PAM-1, and PHM4 cell lines (Fig. 8 B). To overcome these limitations, an inducible expression system for integral membrane PAM was developed using the tetracycline repressor system (Gossen et al., 1993, 1994; Schiller et al., 1997). By regulating the level of PAM expression in the iPAM cell line, we were able to show that the metabolism of membrane PAM is altered as expression levels increase: cleaved PHM products are less prevalent and the soluble products made are stored less well. Individual steps in PAM trafficking, such as internalization from the cell surface, remain to be evaluated.

Maximal expression of PAM in the iPAM cell line was comparable to levels in the anterior pituitary (May et al., 1990) and in cell lines stably transfected with various forms of PAM (Figs. 3 and 4). Before induction, the iPAM cells resembled nontransfected cells in their levels of PAM mRNA, enzyme activity, protein expression, and immunofluorescence. The level of PAM induction observed, when comparing nontransfected cells to maximally expressing iPAM cells, was 20–60-fold depending on the analytical method used. A 35-fold induction of chloramphenicol acetyltransferase was observed using a metallothionein-I promoter in AtT-20 cells, but the requisite levels of divalent metals had toxic effects on the cells (Dickerson et al., 1989). Taken together, these findings highlight the value of this Tet-On cell line in studying the steps in PAM metabolism by regulating its level of expression.

Increasing Expression of PAM-1 Causes Altered Metabolism of PAM-1

rPAM-1 contains several paired basic potential proteolytic cleavage sites and cleavage at the Lys-Lys^{437} site, located within the noncatalytic exon A region, results in separation of the two catalytic domains (Eipper et al., 1993); the 46-kD PHM domain is soluble whereas the 70-kD PAL domain remains membrane bound (Fig. 1; Stoffers et al., 1989). At low levels of PAM-1 expression, a higher proportion of the total PAM is 46-kD PHM and this soluble protein is largely stored in the cells. As levels of PAM-1 expression increase, decreasing amounts of the total PAM are recovered as soluble PHM, and more of the soluble PHM recovered is in the medium. The diminished cleavage of PAM-1 may reflect the fact that less 66-kD PC1ΔC is observed in cell extracts after induction of PAM-1 expression (Fig. 9). PC1 can cleave PAM-1 to soluble PHM and PALm (Marx and Mains, 1997) and PC1ΔC is more active, under the conditions in maturing LDCVs, than is 82-kD PC1 (Zhou and Lindberg, 1994). It is striking that soluble PHM produced from PHM4, a soluble precursor, is efficiently stored whereas soluble PHM produced from membrane PAM-1 is not efficiently stored (Fig. 3 C) (Milgram et al., 1994). Upon induction of PAM-1 expression in the iPAM cells, this phenomenon is replicated.

Increased Expression of Integral Membrane PAM Alters the Regulated Secretory Pathway

The signals mediating the trafficking of soluble, lumenal proteins and membrane proteins from TGN into immature secretory granules (ISGs) and the maturation of secretory granules are not yet understood. Our observation that induction of PAM-1 expression causes dramatic changes in the actin cytoskeleton, eliminates regulated exocytosis, causes the relocalization of soluble lumenal proteins, and limits the cleavage of lumenal proteins, provides new insight into this process. PAM-1 has lumenal and cytosolic components, and both may contribute to the observed effects. We suggest two ways in which membrane PAM could affect the regulated secretory pathway: first, the COOH-terminal domain of PAM may interact with cytosolic factors involved in regulating microtubules and the actin cytoskeleton; second, the lumenal domains of PAM may aggregate with other lumenal proteins (Colomer et al., 1996) (Fig. 11).

A working model for the effect of membrane PAM on the regulated secretory pathway in AtT-20 cells is shown in Fig. 11. The biogenesis of ISGs requires segregation of stored products from proteins leaving via constitutive-like secretion and may involve pH- and Ca^{2+}-dependent selective aggregation (Kuliawat and Arvan, 1992; Kuliawat et al., 1997; Thiele et al., 1997; Kromer et al., 1998) as well as sorting receptors (Cool et al., 1997; Normant and Loh, 1998). Soluble proteins (ACTH, PC1, and soluble PHM) will aggregate as a function of the pH and [Ca^{2+}] in the ISGs (Chanat et al., 1991; Colomer et al., 1996; Thiele et al.,

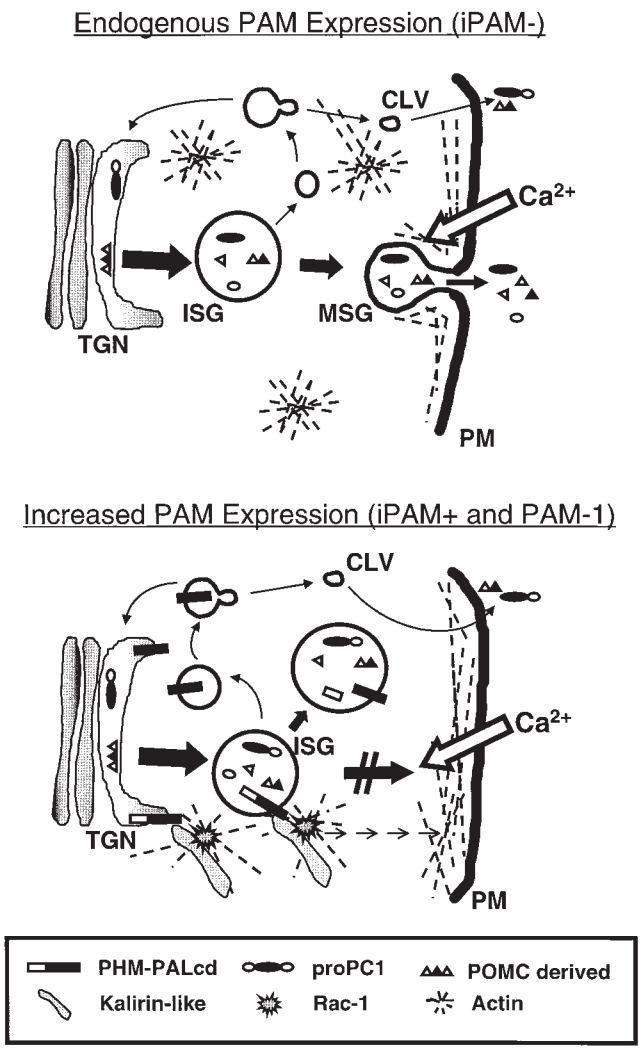

Figure 11. Model for the effects of increased PAM expression in AtT-20 cells. In noninduced iPAM cells (iPAM−) neuroendocrine-specific cleavages begin to occur in ISGs. Products are stored in mature granules (MSGs). Addition of secretagogue stimulates Ca^{2+} entry (mimicked here by addition of Ba^{2+}) and secretion from mature, but not from immature, secretory granules. Budding from ISGs allows nonaggregated content proteins and membrane proteins to leave the ISG and undergo secretion via constitutive-like vesicles (CLV) or return to the TGN. Filamentous actin is scattered throughout the cell. Upon expression of PAM-1 (iPAM+ or PAM-1), the actin cytoskeleton is reorganized and concentrated more at the plasma membrane (PM). Mature granules are no longer collected at the tips of cell processes, regulated exocytosis no longer occurs, and cleavage of secretory granule content proteins is slowed. The interaction of the cytosolic domain of PAM-1 with an endogenous Kalirin-like protein and thus with Rac1 is postulated to cause the observed alterations in the actin cytoskeleton. Inhibition of regulated exocytosis and secretory granule maturation and localization may involve contributions from the lumenal domains of PAM as well as the cytosolic domain.

1997). The extent of proteolytic processing may affect the ability of the proteins to aggregate (Quinn et al., 1991). In cells expressing only endogenous PAM (nontransfected, pUHD, and iPAM−) or PHM4, the prominent granular staining for ACTH and PC1 in the cellular processes (Figs. 6, 7, and 9) and the stimulation of ACTH secretion (Fig. 8 A) indicate that these soluble proteins are sorted into the regulated secretory pathway and stored in mature secretory granules (Mains and May, 1988; Schnabel et al., 1989; Milgram et al., 1994).

ISGs are situated near the TGN and clathrin-coated regions are commonly seen on them, while mature secretory granules lack clathrin-coated regions and are localized to the periphery of the cell (Tooze and Tooze, 1986; Tooze et al., 1991; Dittie et al., 1996; Klumperman et al., 1998). During the process of maturation, secretory granules become responsive to secretagogue addition; this process may involve removal of some proteins and addition of others. Retrieval of furin from ISGs involves AP-1 adaptors and clathrin (Dittie et al., 1997). Similarly, PAM-1 may be retrieved from ISGs through interactions with coat proteins. Since very little PAM-1 appears on the cell surface, whereas a significant amount of soluble PHM undergoes constitutive-like secretion, the soluble and membrane proteins leaving the ISGs must enter a compartment that allows them to part company (Fig. 11).

One of the most dramatic effects of PAM-1 expression is alteration of the actin cytoskeleton. The cytosolic domain of PAM is known to interact with Kalirin, a GDP/GTP exchange factor for Rac1 (Alam et al., 1997). When expressed in fibroblasts, Kalirin disrupts actin stress fibers and dramatically alters cell morphology (Mains et al., 1998). Although expression of Kalirin is restricted to the nervous system in the adult rat, we postulate the existence of a Kalirin-like protein in AtT-20 cells. PAM-1, through its interaction with this Kalirin-like protein, could activate Rac1, a known effector of the actin cytoskeleton (Lamaze et al., 1997; Bellanger et al., 1998). Changes in filamentous actin can enhance or inhibit exocytosis (Muallem et al., 1995; Carbajal and Vitale, 1997; Baldini et al., 1998). In addition, the cytosolic domain of PAM interacts with P-CIP2, a serine/threonine protein kinase expressed in AtT-20 cells, that phosphorylates stathmin, a cytosolic protein known to regulate microtubule stability (Curmi et al., 1997).

Another dramatic effect of expressing PAM-1 is the complete elimination of the ability of AtT-20 cells to secrete in response to addition of secretagogue; this effect was observed in the iPAM cells and in the stably transfected PAM-1 cells (Fig. 8, A and C). Expression of soluble PHM4 did not impair the ability of AtT-20 cells to respond to secretagogue. The altered polymerization of actin may contribute to this effect in several different ways. First, the more extensive network of polymerized actin in the subplasma membrane region may serve as a physical barrier to exocytosis. Second, the altered cytoskeletal organization observed in cells expressing membrane PAM may be responsible for the failure of secretory granules to accumulate in cell processes, in a position from which exocytosis is possible. While it is clear that ISGs cannot respond to secretagogue as well as mature secretory granules, the mechanisms underlying acquisition of secretagogue responsiveness are not clear. Overexpression of PAM-1 may also impair this process.

Induction of PAM-1 expression in iPAM cells and overexpression of PAM-1 in stably transfected cells both result

in the impaired endoproteolytic cleavage of POMC, PC1, and PAM itself, yielding a lumenal compartment full of partially cleaved products (POMC data not shown here; Mains et al., 1991). Maturation of the lumenal contents of the ISG is impaired. Expression of soluble PHM4 does not impair cleavage of lumenal content proteins or storage of ACTH and PC1 in vesicles that accumulate at the tips of cell processes. This effect of PAM-1 could involve both lumenal and cytosolic components. In particular, the ability of the lumenal domains of PAM to aggregate with other lumenal proteins could be important. Although the effects of overexpressing PAM-1 are widespread and diverse, they appear to be focused on the regulated secretory pathway. Localization of endogenous membrane proteins identifying the TGN (TGN38), lysosomes (LAMP1), or endosomes (mannose-6-phosphate receptor) is not dramatically altered in iPAM+ or PAM-1 cells (data not shown).

The dramatic effects of inducing PAM-1 expression in a single cell line demonstrate how well the endoproteolytic events in the lumen of the secretory granules are integrated with the maturation of ISGs and regulated exocytosis. The importance of the cytoskeleton to each of these processes is also apparent. The inducible iPAM cell line should allow us to identify the signaling pathways linking PAM-1 to the cytoskeleton, the manner in which expression of PAM-1 blocks regulated exocytosis, and the steps in the trafficking of PAM that are saturable.

We thank Drs. Manfred Bujard and Hermann Gossen for the rTet inducible vector system. We gratefully acknowledge Marie Bell and Cathy Caldwell for general laboratory assistance.

This work was supported by National Institutes of Health grants DK32948 (R.E. Mains) and DA10478 (M.R. Schiller). G. Ciccotosto was supported by a fellowship LT-647/97 from the Human Frontiers Science Program Organization.

Received for publication 2 June 1998 and in revised form 4 January 1999.

References

Alam, M.R., R.C. Johnson, D.N. Darlington, T.A. Hand, R.E. Mains, and B.A. Eipper. 1997. Kalirin, a cytosolic protein with spectrin-like and GDP/GTP exchange factor-like domains that interacts with peptidylglycine alpha-amidating monooxygenase, an integral membrane peptide-processing enzyme. *J. Biol. Chem.* 272:12667–12675.

Baldini, G., G. Wang, M. Weber, M. Zweyer, R. Breggi, J.W. Witkin, and A.M. Martelli. 1998. Expression of Rab3D N135I inhibits regulated secretory ACTH in AtT-20 cells. *J. Cell Biol.* 140:305–313.

Bellanger, J.M., J.B. Lazaro, S. Diriong, A. Fernandez, N. Lamb, and A. Debant. 1998. The two guanine nucleotide exchange factor domains of Trio link the Rac1 and the RhoA pathways in vivo. *Oncogene.* 16:147–152.

Benjannet, S., N. Rondeau, R. Day, M. Chretien, and N.G. Seidah. 1991. PC1 and PC2 are proprotein convertases capable of cleaving proopiomelanocortin at distinct pairs of basic residues. *Proc. Natl. Acad. Sci. USA.* 88:3564–3568.

Bloomquist, B.T., and R.E. Mains. 1993. The eukaryotic prohormone-processing endoproteases. *Cell Physiol. Biochem.* 3:197–212.

Bloomquist, B.T., B.A. Eipper, and R.E. Mains. 1991. Prohormone-converting enzymes: regulation and evaluation of function using antisense RNA. *Mol. Endocrinol.* 5:2014–2024.

Carbajal, M.E., and M.L. Vitale. 1997. The cortical actin cytoskeleton of lactotropes as an intracellular target for the control of prolactin secretion. *Endocrinology.* 138:5374–5384.

Chanat, E., S.W. Pimplikar, J.C. Stinchcombe, and W.B. Huttner. 1991. What the granins tell us about the formation of secretory granules in neuroendocrine cells. *Cell Biophys.* 19:85–91.

Colomer, V., G.A. Kicska, and M.J. Rindler. 1996. Secretory granule content proteins and the luminal domains of granule membrane proteins aggregate *in vitro* at mildly acidic pH. *J. Biol. Chem.* 271:48–55.

Cool, D.R., E. Normant, F.S. Shen, H.C. Chen, L. Pannell, Y. Zhang, and Y.P. Loh. 1997. Carboxypeptidase E is a regulated secretory pathway sorting receptor: genetic obliteration leads to endocrine disorders in Cpe/*fat* mice. *Cell.* 88:73–83.

Curmi, P.A., S.S.L. Anderson, S. Lachkar, O. Gavet, E. Karsenti, M. Knossow, and A. Sobel. 1997. The stathmin/tubulin interaction in vitro. *J. Biol. Chem.* 272:25029–25036.

Dickerson, I.M., K.W. Peden, and R.E. Mains. 1989. Metallothionein-I promoter-directed expression of foreign proteins in a mouse pituitary corticotrope tumor cell line. *Mol. Cell Endocrinol.* 64:205–212.

Dittie, A.S., N. Hajibagheri, and S.A. Tooze. 1996. The AP-1 adaptor complex binds to immature secretory granules from PC12 cells, and is regulated by ADP-ribosylation factor. *J. Cell Biol.* 132:523–536.

Dittie, A.S., L. Thomas, G. Thomas, and S.A. Tooze. 1997. Interaction of furin in immature secretory granules from neuroendocrine cells with the AP-1 adaptor complex is modulated by casein kinase II phosphorylation. *EMBO (Eur. Mol. Biol. Organ.) J.* 16:4859–4870.

Eipper, B.A., S.L. Milgram, E.J. Husten, H.Y. Yun, and R.E. Mains. 1993. Peptidylglycine α-amidating monooxygenase: a multifunctional protein with catalytic, processing, and routing domains. *Protein Sci.* 2:489–497.

Eskeland, N.L., A. Zhou, T.Q. Dinh, H. Wu, R.J. Parmer, R.E. Mains, and D.T. O'Connor. 1996. Chromogranin A processing and secretion: specific role of endogenous and exogenous prohormone convertases in the regulated secretory pathway. *J. Clin. Invest.* 98:148–156.

Gossen, M., A.L. Bonin, and H. Bujard. 1993. Control of gene activity in higher eukaryotic cells by prokaryotic regulatory elements. *Trends Biochem. Sci.* 18:471–475.

Gossen, M., A.L. Bonin, S. Freundlieb, and H. Bujard. 1994. Inducible gene expression systems for higher eukaryotic cells. *Curr. Opin. Biotechnol.* 5:516–520.

Hendy, G.N., H.P.J. Bennett, B.F. Gibbs, C. Lazure, R. Day, and N.G. Seidah. 1995. Proparathyroid hormone is preferentially cleaved to parathyroid hormone by the prohormone convertase furin. *J. Biol. Chem.* 270:9517–9525.

Husten, E.J., and B.A. Eipper. 1991. The membrane-bound bifunctional peptidylglycine alpha-amidating monooxygenase protein. Exploration of its domain structure through limited proteolysis. *J. Biol. Chem.* 266:17004–17010.

Huttner, W.B., M. Ohashi, R.H. Kehlenbach, F.A. Barr, R. Bauerfeind, O. Braunling, D. Corbeil, M. Hannah, H.A. Pasolli, A. Schmidt, et al. 1995. Biogenesis of neurosecretory vesicles. *Cold Spring Harbor Symp. Quant. Biol.* 60:315–327.

Irminger, J.C., C.B. Verchere, K. Meyer, and P.A. Halban. 1997. Proinsulin targeting to the regulated pathway is not impaired in carboxypeptidase E-deficient Cpe*fat* mice. *J. Biol. Chem.* 272:27532–27534.

Klumperman, J., R. Kuliawat, J.M. Griffith, H.J. Geuze, and P. Arvan. 1998. Mannose 6-phosphate receptors are sorted from immature secretory granules via adaptor protein AP-1, clathrin, and syntaxin 6-positive vesicles. *J. Cell Biol.* 141:359–371.

Kolhekar, A.S., R.E. Mains, and B.A. Eipper. 1997. Peptidylglycine alpha-amidating monooxygenase: an ascorbate-requiring enzyme. *Methods Enzymol.* 279:35–43.

Kromer, A., M.M. Glombik, W.B. Huttner, and H.H. Gerdes. 1998. Essential role of the disulfide-bonded loop of chromogranin B for sorting to secretory granules is revealed by expression of a deletion mutant in the absence of endogenous granin synthesis. *J. Cell Biol.* 140:1331–1346.

Kuliawat, R., and P. Arvan. 1992. Protein targeting via the "constitutive like" secretory pathway in isolated pancreatic islets: passive sorting in the immature granule compartment. *J. Cell Biol.* 118:521–529.

Kuliawat, R., J. Klumperman, T. Ludwig, and P. Arvan. 1997. Differential sorting of lysosomal enzymes out of the regulated secretory pathway in pancreatic β cells. *J. Cell Biol.* 137:595–608.

Lamaze, C., L.M. Fujimoto, H.L. Yin, and S.L. Schmid. 1997. The actin cytoskeleton is required for receptor-mediated endocytosis in mammalian cells. *J. Biol. Chem.* 272:20332–20335.

Leube, R.E., U. Leimer, C. Grund, W.W. Franke, N. Harth, and B. Wiedenmann. 1994. Sorting of synaptophysin into special vesicles in nonneuroendocrine epithelial cells. *J. Cell Biol.* 127:1589–1601.

Lindberg, I., and Y. Zhou. 1995. Overexpression of neuropeptide precursors and processing enzymes. *Methods Neurosci.* 23:94–108.

Mains, R.E., and B.A. Eipper. 1981. Coordinate, equimolar secretion of smaller peptide products derived from pro-ACTH/endorphin by mouse pituitary tumor cells. *J. Cell Biol.* 89:21–28.

Mains, R.E., and B.A. Eipper. 1984. Secretion and regulation of two biosynthetic enzyme activities by mouse corticotropic tumor cells. *Endocrinology.* 115:1683–1690.

Mains, R.E., and V. May. 1988. The role of a low pH intracellular compartment in the processing, storage, and secretion of ACTH and endorphin. *J. Biol. Chem.* 263:7887–7894.

Mains, R.E., B.T. Bloomquist, and B.A. Eipper. 1991. Manipulation of neuropeptide biosynthesis through the expression of antisense RNA for peptidylglycine α-amidating monooxygenase. *Mol. Endocrinol.* 5:187–193.

Mains, R.E., M.R. Alam, R.C. Johnson, D.N. Darlington, N. Bäck, T.A. Hand, and B.A. Eipper. 1998. Kalirin, a multifunctional PAM COOH-terminal domain interactor protein, affects cytoskeletal organization and ACTH secretion from AtT-20 cells. *J. Biol. Chem.* In press.

Marx, R., and R.E. Mains. 1997. Adenovirally encoded prohormone convertase-1 functions in atrial myocyte large dense core vesicles. *Endocrinology.* 138:5108–5118.

May, V., L. Ouafik, B.A. Eipper, and K.M. Brass. 1990. Immunocytochemical

and in situ hybridization studies of peptidylglycine alpha-amidating monooxygenase in pituitary gland. *Endocrinology.* 127:358–364.
Milgram, S.L., R.C. Johnson, and R.E. Mains. 1992. Expression of individual forms of peptidylglycine alpha-amidating monooxygenase in AtT-20 cells: endoproteolytic processing and routing to secretory granules. *J. Cell Biol.* 117:717–728.
Milgram, S.L., R.E. Mains, and B.A. Eipper. 1993. COOH-terminal signals mediate the trafficking of a peptide processing enzyme in endocrine cells. *J. Cell Biol.* 121:23–36.
Milgram, S.L., B.A. Eipper, and R.E. Mains. 1994. Differential trafficking of soluble and integral membrane secretory granule-associated proteins. *J. Cell Biol.* 124:33–41.
Milgram, S.L., S.T. Kho, G.V. Martin, R.E. Mains, and B.A. Eipper. 1997. Localization of integral membrane peptidylglycine alpha-amidating monooxygenase in neuroendocrine cells. *J. Cell Sci.* 110:695–706.
Muallem, S., K. Kwiatkowska, X. Xu, and H.L. Yin. 1995. Actin filament disassembly is a sufficient final trigger for exocytosis in nonexcitable cells. *J. Cell Biol.* 128:589–598.
Natori, S., and W.B. Huttner. 1996. Chromogranin B (secretogranin I) promotes sorting to the regulated secretory pathway of processing intermediates derived from a peptide hormone precursor. *Proc. Natl. Acad. Sci. USA.* 93:4431–4436.
Normant, E., and Y.P. Loh. 1998. Depletion of carboxypeptidase E, a regulated secretory pathway sorting receptor, causes misrouting and constitutive secretion of proinsulin and proenkephalin, but not chromogranin A. *Endocrinology.* 139:2137–2145.
Paquet, L., F. Bergeron, A. Boudreault, N.G. Seidah, M. Chretien, M. Mbikay, and C. Lazure. 1994. The neuroendocrine precursor 7B2 is a sulfated protein proteolytically processed by a ubiquitous furin-like convertase. *J. Biol. Chem.* 269:19279–19285.
Paquet, L., A. Zhou, E.Y. Chang, and R.R. Mains. 1996. Peptide biosynthetic processing: distinguishing prohormone convertases PC1 and PC2. *Mol. Cell Endocrinol.* 120:161–168.
Patel, Y.C., and A. Galanopoulou. 1995. Processing and intracellular targeting of prosomatostatin-derived peptides: the role of mammalian endoproteases. *Ciba. Found. Symp.* 190:26–50.
Quinn, D., L. Orci, M. Ravazzola, and H.P. Moore. 1991. Intracellular transport and sorting of mutant human proinsulins that fail to form hexamers. *J. Cell Biol.* 113:987–996.
Rouille, Y., S.J. Duguay, K. Lund, M. Furuta, Q. Gong, G. Lipkind, A.A. Oliva, Jr., S.J. Chan, and D.F. Steiner. 1995. Proteolytic processing mechanisms in the biosynthesis of neuroendocrine peptides: the subtilisin-like proprotein convertases. *Front. Neuroendocrinol.* 16:322–361.
Schiller, M.R., R.E. Mains, and B.A. Eipper. 1997. A novel neuroendocrine intracellular signaling pathway. *Mol. Endocrinol.* 11:1846–1857.
Schnabel, E., R.E. Mains, and M.G. Farquhar. 1989. Proteolytic processing of pro-ACTH/endorphin begins in the Golgi complex of pituitary corticotropes and AtT-20 cells. *Mol. Endocrinol.* 3:1223–1235.
Seidah, N.G., R. Day, and M. Chretien. 1993. The family of pro-hormone and pro-protein convertases. *Biochem. Soc. Trans.* 21:685–691.
Shen, F.S., and Y.P. Loh. 1997. Intracellular misrouting and abnormal secretion of adrenocorticotropin and growth hormone in cpefat mice associated with a carboxypeptidase E mutation. *Proc. Natl. Acad. Sci. USA.* 94:5314–5319.
Steiner, D.F., Y. Rouille, Q. Gong, S. Martin, R. Carroll, and S.J. Chan. 1996. The role of prohormone convertases in insulin biosynthesis: evidence for inherited defects in their action in man and experimental animals. *Diabetes Metab.* 22:94–104.
Stoffers, D.A., C.B.-R. Green, and B.A. Eipper. 1989. Alternative mRNA splicing generates multiple forms of peptidyl-glycine α-amidating monooxygenase in rat atrium. *Proc. Natl. Acad. Sci. USA.* 86:735–739.
Thiele, E.A., and B.A. Eipper. 1990. Effect of secretagogues on components of the secretory system in AtT-20 cells. *Endocrinology.* 126:809–817.
Thiele, C., H.H. Gerdes, and W.B. Huttner. 1997. Protein secretion: puzzling receptors. *Curr. Biol.* 7:R496–R500.
Thomas, L., R. Leduc, B.A. Thorne, S.P. Smeekens, D.F. Steiner, and G. Thomas. 1991. Kex2-like endoproteases PC2 and PC3 accurately cleave a model prohormone in mammalian cells: evidence for a common core of neuroendocrine processing enzymes. *Proc. Natl. Acad. Sci. USA.* 88:5297–5301.
Tooze, J., and S.A. Tooze. 1986. Clathrin-coated vesicular transport of secretory proteins during the formation of ACTH-containing secretory granules in AtT20 cells. *J. Cell Biol.* 103:839–850.
Tooze, S.A., T. Flatmark, J. Tooze, and W.B. Huttner. 1991. Characterization of the immature secretory granule, an intermediate in granule biogenesis. *J. Cell Biol.* 115:1491–1503.
Udupi, V., P. Gomez, L. Song, O. Varlamov, J.T. Reed, E.H. Leiter, L.D. Fricker, and G.H. Greeley. 1997. Effect of carboxypeptidase E deficiency on progastrin processing and gastrin mRNA expression in mice with the fat mutation. *Endocrinology.* 138:1959–1963.
Varlamov, O., L.D. Fricker, H. Furukawa, D.F. Steiner, S.H. Langley, and E.H. Leiter. 1997. β-cell lines derived from transgenic Cpe*fat* mice are defective in carboxypeptidase E and proinsulin processing. *Endocrinology.* 138:4883–4892.
Vincent, S., L. Marty, and P. Fort. 1993. S26 ribosomal protein RNA: an invariant control for gene regulation experiments in eucaryotic cells and tissues. *Nucleic Acids Res.* 21:1498.
Yoon, J., and M.C. Beinfeld. 1997. PC1 is necessary for the formation of CCK-8 in Rin5F and STC-1 cells. *J. Biol. Chem.* 272:9450–9456.
Yun, H.Y., R.C. Johnson, R.E. Mains, and B.A. Eipper. 1993. Topological switching of the COOH-terminal domain of peptidylglycine alpha-amidating monooxygenase by alternative RNA splicing. *Arch. Biochem. Biophys.* 301: 77–84.
Zhou, A., B.T. Bloomquist, and R.E. Mains. 1993. The prohormone convertases PC1 and PC2 mediate distinct endoproteolytic cleavages in a strict temporal order during proopiomelanocortin biosynthetic processing. *J. Biol. Chem.* 268:1763–1769.
Zhou, A., and R.E. Mains. 1994. Endoproteolytic processing of proopiomelanocortin and prohormone convertases 1 and 2 in neuroendocrine cells overexpressing prohormone convertases 1 or 2. *J. Biol. Chem.* 269:17440–17447.
Zhou, Y., and I. Lindberg. 1994. Enzymatic properties of carboxyl-terminally truncated prohormone convertase 1 (PC1/SPC3) and evidence for autocatalytic conversion. *J. Biol. Chem.* 269:18408–18413.